ADVANCED MATERIALS
www.advmat.de

Role of Water in Directing Diphenylalanine Assembly into Nanotubes and Nanowires

By *Jangbae Kim, Tae Hee Han, Yong-Il Kim, Ji Sun Park, Jungkweon Choi, David G. Churchill, Sang Ouk Kim,** and *Hyotcherl Ihee**

Nanotubes (NTs) and nanowires (NWs) are typical one-dimensional nanomaterials, which have been used extensively as components in various nanodevices owing to their unique properties that arise from their anisotropic structure.[1,2] NTs that bear hollow tubular space can serve in nanofluidic transport,[3] as nanotemplates/nanoreactors,[4] and as catalyst supports/adsorbents because of their large surface area.[5] NWs with highly rigid mechanical properties may serve in composite reinforcement,[6] colloid liquid-crystal systems,[7] and energy devices.[8] Due to such morphology-dependent properties, much research effort has been devoted to trying to achieve NT and NW morphology control.[9] Self-assembly processes of biological molecules, which allow for building-block[10] arrangements, have facilitated control of the morphologies of NTs[11] and NWs[12a] when assisted by the adjustment of preparative conditions. Such assembly is environmentally benign, which is extremely advantageous for biocompatible applications. Despite the enormous scientific interest in such nanostructural properties and the prospect of utility in current and emerging applications, mechanisms of formation for the observed morphologies based on molecular-scale building-block arrangements are still unclear in many cases due to the lack of atomic-scale structural information.

Given this paucity of mechanistic information, in this Communication we set out to try to better understand the self-assembly of an aromatic dipeptide consisting of two covalently linked phenylalanine units (diphenylalanine), which is a key structural motif in the Alzheimer's β-amyloid polypeptide. This system serves as an excellent model because it has been reported to form well-defined NTs,[11] NWs,[12a] nanoribbons,[12b] and nanovesicles via transition from NTs,[13] and such structural and mechanistic considerations are related to investigations into the potential causes of neurodegenerative diseases in humans. Both NT and NW morphologies are formed by the self-assembly of diphenylalanine molecules, in which many interactions such as hydrogen bonding, aromatic stacking, and electrostatic interactions are involved. Among them, the existence of both intermolecular hydrogen bonds between peptide–peptide and peptide–water molecules[11e] and aromatic interactions ($\pi\ldots\pi$) between aromatic side chains has been reported,[11c] and aromatic interactions were observed to be critical for the formation of amyloid fibrils in Alzheimer's disease.[14] In particular, based on the crystal structure, Görbitz provided the evidence that aromatic stacking of diphenylalanine molecules in a hierarchical array surrounding water clusters tightly holds the hydrogen-bonded peptide main chains in NTs; in this way, fibrils are formed along the water channel.[11c] Further, Gazit et al. investigated the dynamics of nanotube assembly from diphenylalanine using NMR spectroscopy;[11b] this study revealed that in NT formation, diphenylalanine molecules migrate out of their water solvation shells to form aggregates, reflected by a decrease in the integral of the diphenylalanine signal and a concomitant increase in the integral of the water signal. Thus, this is known as a nucleation-dependent process, common for highly ordered self-assembly processes. As this example shows, a structural investigation of nano/microscale morphologies on the molecular level can provide important clues in the understanding of the phenomenon of morphological evolution.

In this Communication, we demonstrate that NW morphologies can be obtained by using diphenylalanine in the aqueous phase at high ionic strength. The prepared NWs can then be readily disintegrated and used to form NTs by adjusting the aqueous conditions of preparation. The prepared morphologies of both NWs and NTs are analyzed on the molecular level by using Rietveld[15] refinement of powder X-ray diffraction (PXRD) patterns and subsequently the maximum entropy method (MEM), which reveals an interesting fact that the spatial arrangements of diphenylalanine in both morphologies are closely related to central water clusters via intermolecular hydrogen bonds. Atomic-scale differences between NT and NW morphologies are observed appreciably only in the *a* and *b* directions as the expansion (5.5% from NT to NW) of the hydrophilic channel that encloses the central water column (between N2···N2), whereas the aromatic stacking distance along the *c* direction shows a considerably smaller change (0.1% contraction from NT to NW). Combining the information about

[*] Prof. H. Ihee, J. Kim, Dr. J. Choi
Center for Time-Resolved Diffraction, Department of Chemistry
Graduate School of Nanoscience & Technology (WCU), KAIST
335 Gwahangno, Yuseong-gu
Daejeon, 305-701 (Republic of Korea)
E-mail: hyotcherl.ihee@kaist.ac.kr
Prof. S. O. Kim, T. H. Han, J. S. Park
Department of Materials Science and Engineering (BK21)
KAIST Institute for the Nanocentury, KAIST
335 Gwahangno, Yuseong-gu
Daejeon, 305-701 (Republic of Korea)
E-mail: sangouk.kim@kaist.ac.kr
Dr. Y. Kim
Korea Research Institute of Standards and Science
P.O. Box 102, Yuseong-gu
Daejeon, 305-340 (Republic of Korea)
Prof. D. G. Churchill
Molecular Logic Gate Laboratory, Department of Chemistry, KAIST
335 Gwahangno, Yuseong-gu
Daejeon, 305-701 (Republic of Korea)

DOI: 10.1002/adma.200901973

preparation conditions and structural details on the molecular level may prove helpful in tracking the formation mechanism of each morphology. On the basis of our findings, as well as those from Gazit et al.,[11b] the formation of NWs and NTs seems to be under kinetic and thermodynamic control, respectively, in that each morphology could be prepared depending on the free-water contents in the reaction medium. Indeed, increasing the concentration of diphenylalanine relative to the available water concentration led to the formation of NWs whereas decreasing the concentration led to the formation of NTs. The thermal stability of NTs over NWs from thermogravimetric analysis (TGA) data also clearly supports those features. We believe that the free-water content plays an important role in the self-assembly of diphenylalanine molecules into NTs and NWs.

The synthetic procedure for the aqueous formation of NTs and NWs is illustrated in Figure 1 and is described as follows: diphenylalanine is dissolved in trifluoroacetic acid (TFA) solution, which yields a transparent solution. Thereafter, a NH_4OH solution is slowly added to the reaction mixture under vigorous stirring. When the pH of the reaction mixture approaches the isoelectric (pI) value of 5.5, the solution becomes highly turbid, indicating a rapid assembly of diphenylalanine into NWs. The presence of NWs was confirmed by scanning electron microscopy (SEM). The production of NWs at the pI value suggests that electrostatic interaction via deprotonation of the carboxylic acid functional group may play a crucial role in the self-assembly. Unlike NWs, NTs are prepared simply by sonication and subsequent annealing in deionized water at low concentrations of diphenylalanine. At high diphenylalanine concentrations (>2.5 mg mL^{-1}), NWs rather than NTs are formed as the major product. Notably, the morphological evolution between NTs and NWs is interconvertible in a sense: the dried NWs can be converted into NTs by sonication and annealing in deionized water. Conversely, the NWs can be readily prepared from dried NTs by dissolving NTs in TFA and titrating the sample with NH_4OH. The morphological evolution was confirmed by SEM and is shown schematically in Figure S1 (Supporting Information).

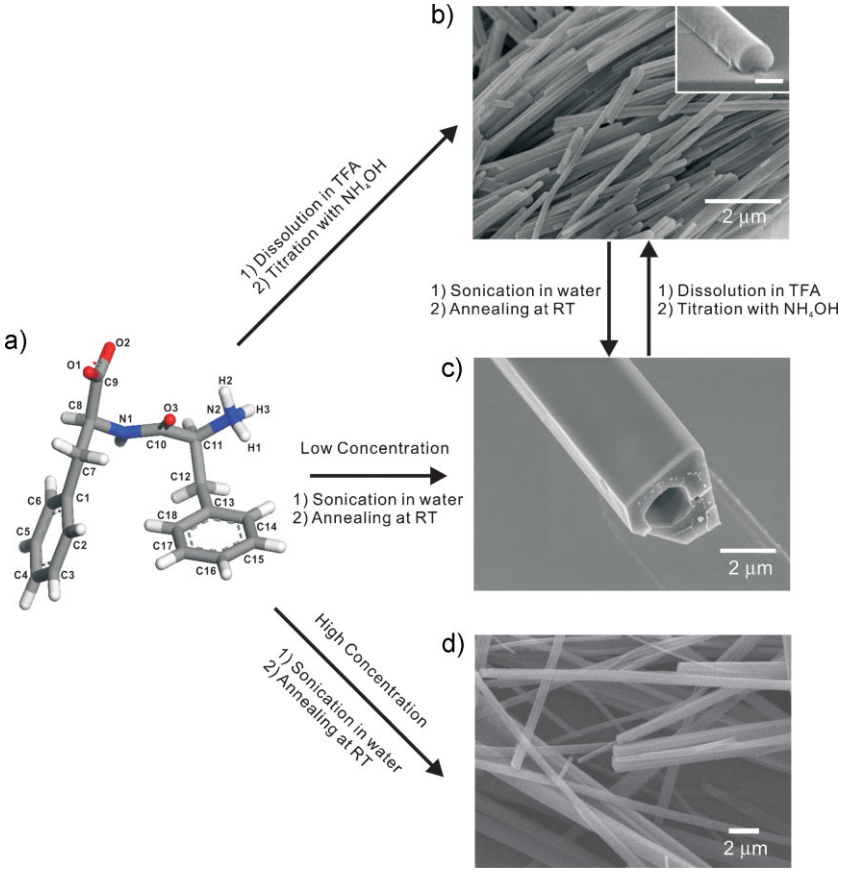

Figure 1. Preparation of NTs and NWs from diphenylalanine and their respective morphology conversion. a) The molecular structure of diphenylalanine from the known single-crystal structure with atomic numbering [11e]. Grey, white, red, and blue portions represent carbon, hydrogen, oxygen, and nitrogen atoms, respectively. b) NWs prepared by the titration method. During titration, a white precipitate was formed near the isolectric condition. Scale bar of inset: 200 nm. c) NTs prepared from low concentration (<~2.5 mg mL^{-1}) of diphenylalanine by sonication and annealing in neutral deionized water. d) NWs prepared from high concentration (>~2.5 mg mL^{-1}) of diphenylalanine by sonication and annealing in neutral deionized water. The threshold concentration of diphenylalanine is around 2.5 mg mL^{-1}. NWs and NTs can be prepared selectively by adjusting the reaction conditions.

To obtain PXRD data, samples of NTs and NWs were prepared by drying the dispersions and finely grinding the residual powder. The PXRD data were collected at room temperature (RT); detailed experimental conditions and structural parameters are provided in Table S1 (Supporting Information). Pawley refinements[16] were performed to optimize the lattice parameters and Rietveld refinements (Fig. 2) in considering all possible geometrical degrees of freedom by using the single-crystal structure of diphenylalanine.[11e] A superposition of the refined structures (Fig. 3a and 3b) clearly reveals that the NW diphenylalanine molecules are translationally shifted away from the central water molecules, compared with those for the NT. The most prominent differences are found in the region between the amine hydrogen atoms at the *N*-terminus of diphenylalanine and the oxygen atoms of water (Fig. 3c and 3d). Four distinct intermolecular hydrogen bonds (HB1–4) are detected in this region; internuclear distances are listed in Table S2 (Supporting Information). Since the strength of intermolecular hydrogen bonds is a function of distance, the increased interaction distances in NWs, relative to the those in the NTs, suggest a generalized weakening of hydrogen bonds in NWs, which may be compensated for by increased electrostatic interaction.

To account for the differences in hydrogen bonding interactions in detail, an electron density map was constructed through MEM analysis for the Rietveld refinement results (Fig. 4). Figure 4a and c represents electron-density distributions for the (001) plane for NTs and NWs, respectively. In these (001) slices, amine nitrogen atoms of the diphenylalanine in NTs and NWs are cleaved at values of

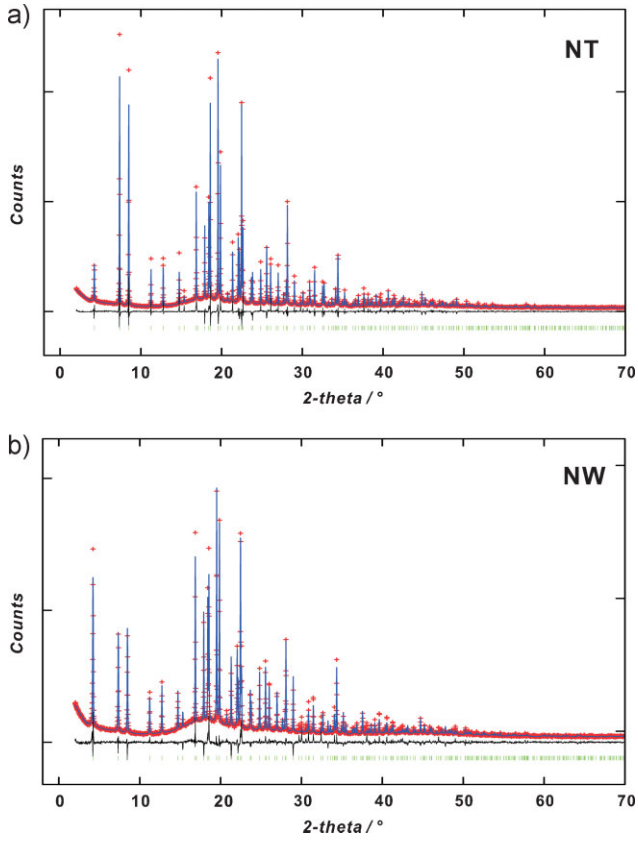

Figure 2. Rietveld refinement patterns for a) NTs and b) NWs using PXRD data at 300 K. Plus (+) marks represent the observed intensities, and the solid line defines calculated ones. A difference (obs. − calc.) plot (black) is shown beneath. Green tick marks below the difference plot indicate the reflection positions.

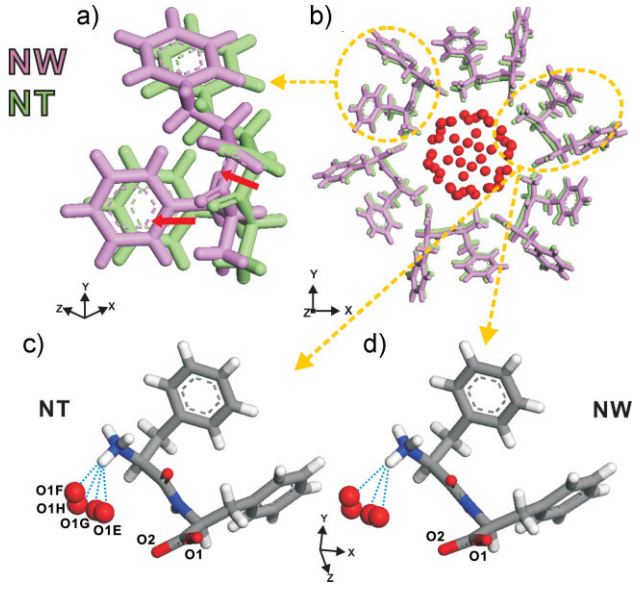

Figure 3. A comparison of the molecular arrangements of diphenylalanine in NTs and NWs in the hexagonal lattice system after Rietveld refinement. a) Superimposed molecular structures of NTs (green) and NWs (magenta); visualization of the relative translational shift (red arrows) of diphenylalanine molecules is shown. b) Superimposed hexagonal array structure of NTs and NWs viewed along the *c* axis. Red solid circles represent central water molecules of arbitrary size; hydrogen atoms are omitted. c) Intermolecular hydrogen bonds (blue dotted lines, within 2.5 Å) between the diphenylalanine and water molecules in NTs. d) Intermolecular hydrogen bonds in NWs.

$z = 0.794$ (NTs) and $z = 0.935$ (NWs), which are fractional coordinates of corresponding nitrogen atoms along the z direction. The nitrogen atom of the amine group and the oxygen atoms of the water, involved in intermolecular hydrogen bonding, are indicated with black 'N' and 'O' labels. The electron density associated with hydrogen bonds in the NTs is about 3.5 times higher than that in the NWs, which is consistent with the notion that NTs have more closely packed 2D contours about the hydrogen bonds than NWs do. In addition, 2D contours around the water molecule (dotted grey circle) also show higher electron densities for NTs than for NWs. Figure 4b and 4d represents electron-density distributions on the (110) plane for NTs and NWs, respectively. Two unit cells elongated (×2) in the *c* direction are shown for better visualization. In these (110) slices, hydrogen bonds are cleaved by the (110) plane, which is 19.5 Å away from the lattice origin. Black arrows indicate the electron density of hydrogen bonds (dotted black rectangle). From the viewpoint of the (110) slices, the electron densities in the NTs are also confirmed to be about 3 times higher than those in the NWs. This difference is true even when the distance of (110) slices is scanned from 19.0 to 20.0 Å. Interestingly, the reduced electron densities of hydrogen bonds in NWs are likely to be closely related to the significantly reduced occupancy in one water oxygen atom (O1G). The occupancy value of O1G is close to 0 for the NWs after Rietveld refinement; therefore, only half the hydrogen bonds seem to be effective when considering occupancy and distance factors. The total occupancies of water oxygen atoms in one asymmetric unit of NWs are ~20% less than those of NTs: the total water oxygen atom occupancy in one asymmetric unit of NWs and NTs is 2.22 and 2.76, respectively.

Besides hydrogen bonds between a diphenylalanine and a water molecule, NTs show stronger hydrogen bonds than NWs in another hydrogen bond motif, namely, the $-NH_2-H\cdots OOC-$ head-to-tail chains formed between two diphenylalanine molecules. This type of hydrogen bond encloses central water molecules in forming a helical architecture with its hydrophilic parts (for both NTs and NWs). Figure S2a and S2b (Supporting Information) reveals this architecture of NTs in the $[0\bar{1}0]$ direction. There are three hydrogen bonds (HB5–7, Table S2, Supporting Information) in which the O1 atom of the carboxylate group serves as a hydrogen bond bridge that interconnects layers (HB6 and HB7), and the O2 atom holds two adjacent diphenylalanine molecules in the same layer (HB5). In the case of NWs, the weakening of one hydrogen bond (HB5) makes a slightly looser lateral packing, wherein the O1 atom is mainly in the hydrogen bonding network between two diphenylalanine molecules. As mentioned previously, aromatic stacking ($\pi\cdots\pi$) between aromatic side chains is also an important driving force in maintaining structural integrity.[11c] However, our results show that the translational shift along the *c* direction from NTs to NWs is negligible (0.1% contraction), and thus both morphologies have nearly the same aromatic stacking distance. The diameter of the

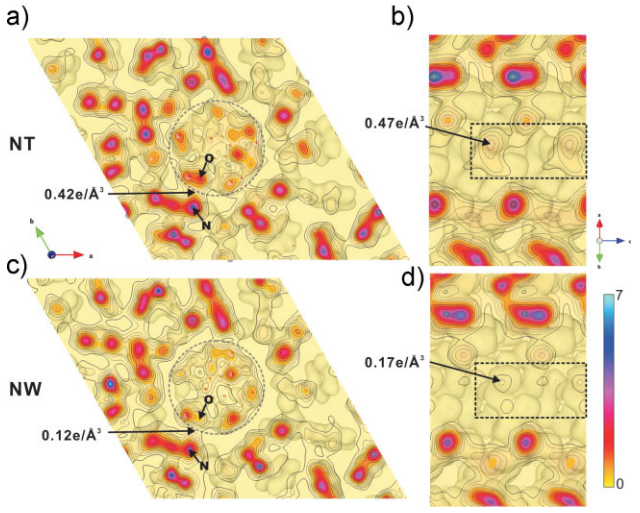

Figure 4. A (001) and (110) slice overlaid with 2D contours illustrating electron-density distribution at a) $z = 0.793$ in NTs, b) 19.5 Å from the lattice origin in NTs, c) $z = 0.935$ in NWs, and d) 19.5 Å from the lattice origin in NWs. Contours are plotted up to 7.0 e Å^{-3} and the isosurface level is 0.5 e Å^{-3}. For a (001) slice, $z = 0.793$ and $z = 0.935$ pass through one nitrogen atom of an amine group in NTs and NWs, respectively. The positions of nitrogen and oxygen atom are denoted by black 'N' and 'O' labels. The area of central water clusters is represented by dotted grey circles. For a (110) slice, the distance of 19.5 Å from the lattice origin corresponds to a halfway point between amine hydrogen atoms and water oxygen atoms. The area of hydrogen bonds cleaved along the (110) plane is represented by dotted black retangles. For a clear visualization of the (110) plane, sliced surface and 2D contours are elongated by two in the *c* direction for clarity. The electron density in NTs associated with hydrogen bonds is about three times higher than that in NWs in both the (001) and (110) slices: 0.42, 0.47 for NTs and 0.12, 0.17 for NWs.

hydrophilic channel that encloses the central water column (between $N_2 \cdots N_2$) is 12.217 and 12.886 Å for NTs and NWs, respectively, indicating a notable expansion (~5.5% from NT to NW) in spacing between the diphenylalanine molecules in the NWs.

To assess the stability in both hierarchical structures, TGA was performed. TGA data reveal a weight loss in the NT sample at around 611 K (Fig. S3a, Supporting Information), attributed to the heat-induced loss of the diphenylalanine moiety from the ordered hexagonal array that constitutes the NTs.[17] In the case of NWs, this temperature is reduced to 594 K (Fig. S3b, Supporting Information), indicating that NWs are thermodynamically less stable than NTs in the absence of solvent. After NWs were formed at the pI condition prepared by adding NH_4OH solution to a TFA solution, NWs could then be converted into NTs under the same buffer condition by sonicating and annealing the prepared NWs in situ. The converted NT morphology was confirmed by SEM measurements. The high ionic strength resulting from initial TFA acid and titrated base appears to direct the formation of NWs, possibly by reducing the free-water content available to self-assembly of diphenylalanine. Interestingly, NWs can be easily prepared even under the same preparation condition of NTs by controlling the concentration of diphenylalanine. Providing a high concentration of diphenylalanine in deionized water and sonicating or heating of this solution leads to the formation of NWs rather than NTs. NWs prepared at high concentration have a high aspect ratio with increased diameter compared with NWs from the titration method (Fig. 1d). The threshold concentration of diphenylalanine is around 2.5 mg mL^{-1}. Under this threshold value, NTs are dominant and vice versa. The prepared morphologies are confirmed by inspection of SEM images. However, the formation of NTs takes a considerably longer time than the formation of NWs. While NWs are formed predominantly above the concentration of 2.5 mg mL^{-1}, gellation is observed from a concentration of 3.0 mg mL^{-1} and bulk water is trapped in the gel matrix at a concentration of 6.0 mg mL^{-1}. As the concentration of diphenylalanine is increased, the time for the formation of NWs is decreased. Based on our observation, concentration-dependent morphological evolution highly suggests that the content of free water in the reaction mixture plays a pivotal role in determining the formation of NTs and NWs.

In summary, we have demonstrated controlled assembly of diphenylalanine molecules to form NWs and NTs as well as providing molecular-scale ordering for each nanoscale morphology. Rietveld refinements of the experimental PXRD patterns reveal that a morphological difference between NTs and NWs is closely related to slight, yet clear, differences in the molecular arrangement of diphenylalanine. The major differences between NTs and NWs are the translational movements of the diphenylalanine molecules in NWs and the two kinds of significantly weakened intermolecular hydrogen bonds in NWs, compared with those in NTs. To explain this quantitatively, electron densities in NTs and NWs were generated by the MEM and cleaved along the (001) and (110) planes parallel/normal to the hydrogen bonds for direct comparison. The electron densities in NTs were approximately three times higher than those for NWs. A comparably lower value for the NWs is consistent with a slight expansion observed along both the *a* and *b* directions, compared with the structural values for the NTs. The higher number of hydrogen bonds in NTs is consistent with a greater observed thermal stability according to TGA results. Finally, lower free-water content caused by high ionic strength or high solute concentration may direct the formation of NWs over the energetically more favorable NTs.

Experimental

Materials: The lyophilized form of the NH_2–Phe–Phe–COOH dipeptide was purchased from Bachem (Bubendorf, Switzerland). Water was deionized by using Milipore MilliQ. NH_3 solution and trifluoroacetic acid were purchased from Junsei Chemical Co. (Japan) and Samchun Pure Chemical Co. (Korea), respectively.

Preparation of Peptide NTs: A deionized water solution of NH_2–Phe–Phe–COOH (diphenylalanine) was prepared (2 mg mL^{-1}) via sonication (20 min) with subsequent annealing (80 °C, 30 min). Peptide NTs were formed during cooling to ambient temperature. When the diphenylalanine molecules are dissolved in deionized water in the preparation of NTs, the pH of the solution approaches the isoelectric point and shows concentration dependence. A solution of diphenylalanine (2 mg mL^{-1}) in deionized water resulted in a pH of approximately 5.3. From this observation, the diphenylalanine molecules in the NTs were also assumed to be in their zwitterionic form.

Preparation of Peptide NWs: A portion of aromatic diphenylalanine was dissolved in trifluoroacetic acid and subsequently titrated by adding a portion of ammonia solution (approx. 30 wt%) to reach the isoelectric

point of pH 5.5. After this titration, the final diphenylalanine concentration in the reaction mixture was 5.26 mg mL^{-1}. NWs could then self-assemble under isoelectric conditions. Excess salt was removed by washing with deionized water.

Control of NT and NW Morpohologies: The independently prepared and dried NTs and NWs could be converted: the NTs could be converted to NWs, and NWs to NTs, by applying respective preparation conditions. Sonicating and annealing of the dispersed NWs in deionized water yielded the NT morphology (Fig. S1a, Supporting Information). Conversely, dissolving the dried NTs in TFA and titrating the solution with NH_4OH solution yielded the NW morphology (Fig. S1b, Supporting Information). In the case of NWs, even this morphological evolution from NWs to NTs was observed under its original buffer condition as follows: NWs can be converted into NTs in situ without changing the reaction medium by sonicating and annealing the reaction mixture.

Scanning Electron Microscopy: The morphology of peptide NTs or NWs was analyzed by a field-emission scanning electron microscope (Hitachi S-4800, Japan). A carbon coating was used to enhance scattering contrast and electric conductivity (CED 030 carbon evaporator, Bal-tec, Germany).

Collection and Refinement of PXRD Patterns: High-resolution PXRD data of NT and NW samples were collected at the 8C2 high-resolution powder diffraction beamline of the Pohang Accelerator Laboratory in Pohang, Korea. The incident X-ray was vertically collimated by a mirror and monochromatized to the wavelength of 1.5489 Å by using a double-crystal Si(111) monochromator. The diffraction patterns were scanned over 2θ values ranging from 2.00° up to 70.00° in increments of 0.02° (room temperature). The samples for PXRD were prepared by evaporating water and fully grinding the remaining powder. The sample holder on the instrument was rotated about a vector normal to the surface during measurement to increase sampling statistics and to reduce preferred orientation effects. The obtained experimental powder diffraction patterns are in good agreement with a simulated powder diffraction pattern of the previously reported single-crystal structural data (CCDC 163340 contains the supplementary crystallographic data for this paper. These data can be obtained free of charge from The Cambridge Crystallographic Data Centre via www.ccdc.cam.ac.uk/data_request/cif) [11e]. With this unit cell structure, we performed Pawley refinement to optimize the lattice parameters iteratively until no change was obtained in the R_{WP} value. The orthogonal polynomials with 20 coefficients were used as the basis set for fitting the experimental background. In Rietveld refinements, the positions and torsional angles of diphenylalanine molecules were explicitly considered as structural degrees of freedom. The March–Dollase function was selected for the preferred orientation correction and an anisotropic temperature factor was applied for all heavy atoms. For water molecules, isotropic temperature factors and occupancies were refined only. Rietveld refinement gave good convergence even when all parameters were refined simultaneously. The final refined parameters are summarized in Table S1 (Supporting Information) and selected intermolecular hydrogen bond distances are listed in Table S2 (Supporting Information). Most of the molecular modeling, Pawley refinements, Rietveld refinements, and electron-density calculations via the MEM were carried out using *Rietan-FP* [18] and *Reflex*, a software package for crystal structure determination from powder diffraction patterns, implemented in MS modeling v4.2 (Accelrys Inc.) [19]. The visualization and analysis of the electron-density map from MEM were performed by using VESTA program [20].

Thermogravimetric Analysis of NTs and NWs: Small amounts of dried samples of each were heated from 303 to 773 K with a constant heating rate of 5 K min^{-1}.

Acknowledgements

This work was supported by Creative Research Initiatives (Center for Time-Resolved Diffraction) of MEST/KOSEF and the National Research Laboratory Program (R0A-2008-000-20057-0) of KOSEF, Republic of Korea. Supporting Information is available online from Wiley InterScience or from the author.

Received: June 9, 2009
Published online: September 11, 2009

[1] a) Y. Xia, P. Yang, Y. Sun, Y. Wu, B. Mayers, B. Gates, Y. Yin, F. Kim, H. Yan, *Adv. Mater.* **2003**, *15*, 353. b) G. R. Patzke, F. Krumeich, R. Nesper, *Angew. Chem.* **2002**, *114*, 2554; *Angew. Chem. Int. Ed.* **2002**, *41*, 2446. c) J. Hu, T. W. Odom, C. M. Lieber, *Acc. Chem. Res.* **1999**, *32*, 435.

[2] a) W. Lu, C. M. Lieber, *Nat. Mater.* **2007**, *6*, 841. b) S. Ju, A. Facchetti, Y. Xuan, J. Liu, F. Ishikawa, P. Ye, C. Zhou, T. J. Marks, D. B. Janes, *Nat. Nanotechnol.* **2007**, *2*, 378. c) J. H. Ahn, H. S. Kim, K. J. Lee, S. Jeon, S. J. Kang, Y. Sun, R. G. Nuzzo, J. A. Rogers, *Science* **2006**, *314*, 1754. d) X. Duan, Y. Huang, R. Agarwal, C. M. Lieber, *Nature* **2003**, *421*, 241.

[3] J. Goldberger, R. Fan, P. Yang, *Acc. Chem. Res.* **2006**, *39*, 239.

[4] W. Han, S. Fan, Q. Li, Y. Hu, *Science* **1997**, *277*, 1287.

[5] F. Cheng, J. Chen, X. Gou, *Adv. Mater.* **2006**, *18*, 2561.

[6] P. Yang, C. M. Lieber, *Science* **1996**, *273*, 1836.

[7] L. S. Li, J. Walda, L. Manna, A. P. Alivisatos, *Nano Lett.* **2002**, *2*, 557.

[8] M. Law, L. E. Greene, J. C. Johnson, R. Saykally, P. Yang, *Nat. Mater.* **2005**, *4*, 455.

[9] a) C. Zhou, J. Han, R. Guo, *J. Phys. Chem. B* **2008**, *112*, 5014. b) X. Zhang, X. Zhang, W. Shi, X. Meng, C. Lee, S. Lee, *Angew. Chem.* **2007**, *119*, 1547; *Angew. Chem. Int. Ed.* **2007**, *46*, 1525. c) I. W. Hamley, *Angew. Chem.* **2007**, *119*, 8274; *Angew. Chem. Int. Ed.* **2007**, *46*, 8128. d) N. Ashkenasy, W. S. Horne, M. R. Ghadiri, *Small*, **2006**, *2*, 99.

[10] a) U. Feldkamp, C. M. Niemeyer, *Angew. Chem.* **2006**, *118*, 1888; *Angew. Chem. Int. Ed.* **2006**, *45*, 1856. b) X. Gao, H. Matsui, *Adv. Mater.* **2005**, *17*, 2037. c) S. Zhang, *Nat. Biotechnol.* **2003**, *21*, 1171. d) N. C. Seeman, *Nature* **2003**, *421*, 427. e) D. T. Bong, T. D. Clark, J. R. Granja, M. R. Ghadiri, *Angew. Chem.* **2001**, *113*, 1016; *Angew. Chem. Int. Ed.* **2001**, *40*, 988.

[11] a) M. Reches, E. Gazit, *Nat. Nanotechnol.* **2006**, *1*, 195. b) O. Carny, D. E. Shalev, E. Gazit, *Nano Lett.* **2006**, *6*, 1594. c) C. H. Görbitz, *Chem. Commun.* **2006**, 2332. d) M. Reches, E. Gazit, *Science* **2003**, *300*, 625. e) C. H. Görbitz, *Chem. Eur. J.* **2001**, *7*, 5153.

[12] a) T. H. Han, J. Kim, J. S. Park, C. B. Park, H. Ihee, S. O. Kim, *Adv. Mater.* **2007**, *19*, 3924. b) T. H. Han, J. K. Oh, J. S. Park, S.-H. Kwon, S.-W. Kim, S. O. Kim, *J. Mater. Chem.* **2009**, *19*, 3512.

[13] a) X. Yan, Y. Cui, Q. He, K. Wang, J. Li, W. Mu, B. Wang, Z. Ou-yang, *Chem. Eur. J.* **2008**, *14*, 5974. b) X. Yan, Q. He, K. Wang, L. Duan, Y. Cui, J. Li, *Angew. Chem.* **2007**, *119*, 2483; *Angew. Chem. Int. Ed.* **2007**, *46*, 2431. c) P. P. Bose, A. K. Das, R. P. Hegde, N. Shamala, A. Banerjee, *Chem. Mater.* **2007**, *19*, 6150.

[14] a) O. S. Makin, E. Atkins, P. Sikorski, J. Johansson, L. C. Serpell, *Proc. Natl. Acad. Sci. USA* **2005**, *102*, 315. b) E. Gazit, *FEBS J.* **2005**, *272*, 5971.

[15] a) For Rietveld refinement: H. M. Rietveld, *J. Appl. Crystallogr.* **1969**, *2*, 65. Reviews for structure determination from PXRD: b) K. D. M. Harris, M. Tremayne, B. M. Kariuki, *Angew. Chem.* **2001**, *113*, 1674; *Angew. Chem. Int. Ed.* **2001**, *40*, 1626. c) K. D. M. Harris, M. Tremayne, *Chem. Mater.* **1996**, *8*, 2554.

[16] G. S. Pawley, *J. Appl. Crystallogr.* **1981**, *14*, 357.

[17] V. L. Sedman, L. Adler-Abramovich, S. Allen, E. Gazit, S. J. B. Tendler, *J. Am. Chem. Soc.* **2006**, *128*, 6903.

[18] F. Izumi, K. Momma, *Solid State Phenom.* **2007**, *130*, 15.

[19] Reflex, Material Studio Release Notes, Release 4.2, Accelrys Software, Accelrys, San Diego **2006**.

[20] K. Momma, F. Izumi, *J. Appl. Crystallogr.* **2008**, *41*, 653.